

1 **Diagnosing land-atmosphere interaction from a**
2 **regional climate model simulation over West-**
3 **Africa**

4
5 Bart JJM van den Hurk

6 Erik van Meijgaard

7 KNMI, PO Box 201, 3730 AE De Bilt

8 Correspondence: hurkvd@knmi.nl

9
10 Version: 17 apr 2009

11
12 To be submitted for publication to J.Hydrometeorology

13
14 **Keywords:** Land-atmosphere interaction; Regional Climate Modeling; African
15 hydrological cycle, recycling ratio, convective triggering potential

16

17 **Abstract**

18 Using a Regional Climate Model (RCM) covering a large area around the West African
19 Sahel land-atmosphere interaction at climatological time scales has been explicitly
20 explored using a range of diagnostics. First, areas and seasons of strong land-
21 atmosphere interaction were diagnosed from the requirement of a combined
22 significant correlation between soil moisture, evaporation and recycling ratio. The
23 northern edge of the West African monsoon area during JJA, and an area just north of
24 the equator (Central African Republic) during MAM were identified. Further analysis in
25 these regions focused on the seasonal cycle of the Lifting Condensation Level (LCL)
26 and the Convective Triggering Potential (CTP), and the sensitivity of CTP and near-
27 surface dewpoint depressions (HI_{low}) to anomalous soil moisture. From these analyses
28 it is apparent that atmospheric mechanisms impose a strong constraint on the impact
29 of soil moisture on the regional hydrological cycle.

30

31 **Introduction**

32 Land-atmosphere interaction is manifest at a wide range of spatial and temporal scales
33 (Van den Hurk and Blyth, 2008). The planetary boundary layer is affected by the
34 evaporation from the surface and changes in the atmospheric humidity affect surface
35 evaporation within a couple of hours. The Lifting Condensation Level (LCL) is strongly
36 coupled to the surface relative humidity and soil moisture (Betts, 2004). The ability of
37 the atmosphere to produce precipitation is partly dependent on surface fluxes affecting
38 convective activity and moisture supply at a similar time scale (Findell and Eltahir,
39 2003a; Taylor and Ellis, 2006). Soil moisture anomalies may affect subsequent rainfall
40 at synoptic (Koster et al. 2000; 2003) or monthly to seasonal (Koster et al. 2004) time
41 scales. Seneviratne et al. (2006) show shifts in regions of strong coupling induced by
42 climate change on multi-decadal time scales. The monthly to seasonal time scale is
43 particularly relevant, as it holds promises for improving seasonal forecasting by
44 exploiting the predictability contained in the soil moisture state (Douville et al. 2009).

45

46 The hydroclimate in areas with a strong annual cycle, like monsoon regions or areas
47 affected by tropical convection, displays strong spatial and temporal gradients of the
48 strength of land-atmosphere interaction at the seasonal time scale. Land-atmosphere
49 interaction and, in particular, anomalous soil moisture under conditions of long soil
50 memory, are held partly responsible for anomalies in the strength or duration of wet or
51 dry episodes in for instance the West-African monsoon area (Koster et al. 2004;
52 Douville et al. 2007).

53

54 Recently, Dirmeyer et al. (2009) developed an elegant framework in which a series of
55 observable correlations are indicative of a strong land-atmosphere interaction and
56 associated predictability. In order to have a strong and predictable atmospheric
57 response to soil moisture anomalies three conditions should be met. First, surface
58 evaporation is positively correlated with soil moisture. Negative correlations point at
59 conditions where evaporation is depleting the soil reservoir and is primarily limited by
60 available energy or atmospheric demand. Second, evaporation is positively correlated
61 with soil memory. This criterion ensures that anomalous wetness conditions are
62 actually remembered in the subsequent period. Third, atmospheric recycling of water
63 is positively correlated with soil moisture. This ensures that the atmosphere is actually
64 responsive to local wetness anomalies, and that precipitation is not entirely driven by
65 remote advection and/or atmospheric circulation. Their analysis based on a mixture of
66 multiyear (surface) model results and observational datasets reveals that only few
67 areas in West Africa show a strong land-atmosphere coupling in either of the main
68 seasons.

69

70 The statistical correlations in the analysis of Dirmeyer et al. (2009) are well interpreted
71 in terms of general behavior of the interacting land-atmosphere system. However, they
72 do not reveal a lot of information on the responsible mechanisms that play a role in
73 this interaction. Dirmeyer et al. (2006) and Guo et al. (2006) address the surface
74 evaporation response to soil moisture and radiation to explain the multi-model spread
75 in the analysis of regions of strong land-atmosphere coupling presented by Koster et
76 al. (2004). A closer look at atmospheric processes is needed to understand and model
77 this complex interaction properly. However, the large number of degrees of freedom in

78 the atmosphere complicates a comprehensive (preferably observation based)
79 experimental set-up aiming at diagnosing the atmospheric control on land-atmosphere
80 interaction. Findell and Eltahir (2003a,b) introduced a framework in which a single-
81 column model was driven by observed atmospheric profiles, and where the sensitivity
82 of convective triggering to soil moisture conditions was evaluated. They presented
83 maps of systematic positive and negative feedbacks over the US, conditioned on the
84 Convective Triggering Potential (CTP) and a measure of the near-surface dewpoint
85 depression (HI_{low}). Betts (2004) carried out a range of evaluations of Global
86 Circulation Model (GCM) outputs focusing at the role of LCL, clouds and radiation on
87 the local land-atmosphere interaction. Also Regional Climate Models (RCMs) have
88 been used by a number of authors to assess the sensitivity of the regional
89 hydroclimate to anomalous moisture conditions. Like the work of Findell and Eltahir
90 (2003b) both positive and negative feedbacks are found depending on the governing
91 conditions and processes (Schär et al. 1999; Kanamitsu and Mo, 2003; Cook et al.
92 2006; Fischer et al. 2007; Bisselink and Dolman, 2008). Most of these studies
93 consider a number of cases, but systematic evaluation of the coupling characteristics
94 at multiyear time scales has hardly been carried out.

95

96 In this study we use a variety of diagnostics to identify the regions and seasonal timing
97 of systematic land-atmosphere interaction in Western Africa on a climatological time
98 scale. This area includes regions of strong coupling as indicated by the work of Koster
99 et al. (2004), and is an ideal testbed for exploring a suite of coupling diagnostics due
100 to strong seasonal and spatial gradients of both land surface and atmospheric
101 processes acting on the moisture budget. Following largely the correlation framework

102 of Dirmeyer et al. (2009) we first identify such regions in a 19-year hind-cast
103 simulation (1989 – 2007) with a Regional Climate Model. Subsequently, we evaluate
104 the sensitivity of a number of atmospheric key properties (LCL, CTP, HI_{low}) playing a
105 role in land-atmosphere coupling to soil moisture conditions. The model used
106 reproduces the observed seasonality in precipitation very well while maintaining
107 sufficient degrees of freedom in the interior to allow realistic land-atmosphere
108 feedback processes. By doing so, we make use of the capability of regional climate
109 modeling in representing land surface and atmospheric processes and their
110 interaction under conditions that are constrained by observed large scale atmospheric
111 boundary conditions.

112

113 In the following we will detail the diagnostics and frameworks. The modeling set-up
114 and the climatological verification are briefly described. After presenting the results on
115 the identified areas and the response of the atmospheric key variables, we will argue
116 that a systematic impact of soil moisture anomalies on local precipitation is strongly
117 constrained by a mixed occurrence of positive and negative feedback processes, and by
118 a strong control of the climatological seasonal cycles of the atmospheric key variables.

119

120 **Definition of diagnostics**

121 For a strong mutual interaction between the surface and the atmosphere both surface
122 evaporation and precipitation must be governed by local moisture conditions. In our
123 set-up we retain two out of the three criteria of Dirmeyer et al. (2009): a collocation of
124 a strong positive anomaly correlation between evaporation and soil moisture, and a
125 strong positive correlation between soil moisture and recycling ratio. The criterion

126 involving a strong correlation between evaporation and soil memory is believed crucial
127 for the potential contribution of soil moisture information to the hydrological
128 predictability at monthly or longer time scales, but a weak correlation does not
129 preclude the existence of a strong interaction at shorter (daily to monthly) time scales.

130

131 *Correlation between daily soil moisture and evaporation*

132 For this study soil moisture W is taken as the model value cumulated over the top 1 m
133 of soil (see model description below). It thus reflects the soil water that can be
134 transported to the atmosphere via vegetation transpiration within a seasonal time
135 scale. The correlation between daily soil moisture W and evaporation E is calculated
136 after removal of the mean seasonal cycle, calculated by averaging each calendar day in
137 the 19-yrs timeseries. No smoothing or spatial filtering was applied to these fields.
138 Monthly averages of anomalies of W and E are used to calculate the correlation
139 coefficients. The significance of the correlation is determined by a one-sided t -test
140 (significance level 95%), where the number of degrees of freedom is determined by
141 the number of valid values within a given averaging period (maximum about 90 days \times
142 19 years for seasonal averages) divided by a measure of the soil moisture memory
143 time scale. This time scale was defined as the time lag at which the soil moisture
144 autocorrelation drops below $1/e$ (the e-folding time scale). For each day in the entire
145 record the autocorrelation was calculated with a backward time lag, and a mean
146 seasonal memory time scale was defined as the average e-folding time scale of all days
147 of each simulation year within that particular season.

148

149 *Correlation between recycling ratio and soil moisture*

150 The recycling ratio was calculated by a “Lagrangian” method (Dominguez et al. 2006),
151 in which for each 6-hourly model output interval with precipitation the moisture
152 budget of a series of upstream model columns was integrated in order to estimate the
153 source area of the precipitation. By vertically integrating the product of the horizontal
154 wind and atmospheric moisture content at each model level a trajectory along which
155 the moisture column q is advected was constructed, pointing at the next upwind
156 model column x . The ratio E/q was integrated over a number of columns until a
157 specified distance L from the originating column was reached. The recycling ratio R
158 can then be shown to be given by (Dominguez et al. 2006; Bisselink and Dolman,
159 2008):

160

161
$$R = 1 - \exp \left[- \int_0^L \frac{E(x)}{\left| \frac{\Delta x}{\Delta t} \right| q(x)} dx \right] \quad (1)$$

162

163 where Δt is the processing time step (6 hours) and Δx the horizontal distance traveled
164 within a time step. The procedure was applied to all 6-hourly intervals in a given
165 month to calculate a monthly recycling ratio. Values of L were varied over a range
166 between 100 and 1000 km. Although the overall value of R increases with L the spatial
167 and temporal pattern of R is fairly insensitive to the choice of L , and values calculated
168 with $L = 500$ km were used. As before, a significant correlation between monthly R and
169 W was determined by a t -test with the number of degrees of freedom set by the

170 number of days in the considered period divided by the soil moisture memory time
171 scale.

172

173 *Definition of regions with significant coupling*

174 A seasonal mean correlation was calculated considering all monthly anomalies of W
175 and monthly values of E and R . The conventional meteorological seasons (DJF, MAM,
176 JJA, SON) were selected for each location, in spite of the fact that at some locations
177 (for instance the northern edge of the West-African monsoon area) the typical annual
178 cycle of succession of dry and wet episodes does not coincide with these time
179 intervals. Areas where both W and E , and W and R show a significantly positive
180 correlation are identified as areas prone to strong land-atmosphere interaction at the
181 climatological time scale. In these areas evaporation is higher when soil moisture is
182 higher, showing a control of soil moisture on evaporation rather than vice versa. Also,
183 a higher recycling ratio for wetter soil conditions points at atmospheric conditions
184 where precipitation is at least partly controlled by the local surface conditions, and not
185 entirely due to remote advection of moisture. A spatial smoothing to the significance
186 levels was applied to yield spatially consistent patterns. Grid points are only
187 considered if for six out of the adjacent 3×3 grid boxes a significant correlation of the
188 same sign is found.

189

190 *Atmospheric properties*

191 For each grid point and each day the Lifting Condensation Level (LCL) is computed
192 from the daily mean air temperature T_2 and dewpoint temperature T_d both at 2m
193 height. The LCL is defined as the intersection of a dry adiabatic lapse rate from T_2 and

194 a moist adiabatic lapse rate from T_d . As it is closely related to the surface relative
195 humidity (Betts, 2004) it generally increases with decreasing soil moisture content.
196 However, this sensitivity is strongly controlled by atmospheric processes affecting the
197 thermodynamic structure of the planetary boundary layer and above.

198

199 The Convective Triggering Potential (CTP) is a measure for the atmospheric ability to
200 trigger convection (Findell and Eltahir, 2003a). It is defined as the vertically integrated
201 early morning (6 UTC) difference between the atmospheric temperature T and the
202 moist adiabatic lapse rate T_m in the range between 100 and 300 hPa above the
203 surface. This range is considered to be critical as surface processes may modulate the
204 LCL and the atmospheric boundary layer (ABL) within this range. During most
205 conditions the ABL will reach 100 hPa above surface, but 300 hPa above surface is
206 rarely exceeded. The moist adiabat is calculated by assuming a saturated parcel ascent
207 from 100 hPa above the surface and accounting for the heat release (and temperature
208 increase) as condensation occurs. The energy released when condensation occurs may
209 be an additional source of buoyancy, possibly triggering free convection depending on
210 the CTP. Negative values of CTP (T on average exceeds T_m) indicate a stably stratified
211 atmosphere in which no convection can occur. Very high CTP-values are indicative of
212 likely occurrence of (wet or dry) free convection.

213

214 A second variable in the framework of Findell and Eltahir (2003a) distinguishes
215 between wet and dry atmospheric conditions, in relation to the formation of
216 precipitation from convective events. They define a humidity index HI_{low} as the sum of
217 the dewpoint depression ($T - T_d$) at 50 and 150 hPa above the surface. Very high

218 values of HI_{low} are indicative of dry conditions in which no precipitation will occur as
219 the air is too far away from saturation. Very low values will very likely produce
220 precipitation, regardless the state of the surface or convective activity.

221

222 In their CTP – HI_{low} framework Findell and Eltahir (2003a) define a set of conditions in
223 which the soil moisture state is likely to influence the occurrence of convective
224 precipitation. In many cases ($CTP < 0$, HI_{low} too low or too high) precipitation is
225 independent of the surface energy partitioning. For relatively low values of HI_{low} and
226 positive CTP precipitation is favored over wet soils as the surface provides a source of
227 moist static energy that can convert into convective precipitation. Wetting an already
228 wet soil implies a positive feedback loop. Note that this positive feedback has a
229 different nature than the positive feedback implied by e.g. d'Andrea et al. (2006) and
230 Bierkens and van den Hurk (2008), which is based on atmospheric moisture budget
231 considerations rather than on the thermodynamic properties of the atmosphere.
232 Under dryer conditions and higher CTP values, convection is favored over dry soils
233 which force the LCL to reach to higher levels, a negative feedback.

234

235 **Set-up and brief verification of the RCM**

236 The RCM considered here is an upgrade of the Regional Atmospheric Climate MOdel
237 (RACMO) version 2.1 (Van Meijgaard et al. 2008). It uses a semi-Lagrangian
238 dynamical formulation and the physical parameterization of the European Centre for
239 Medium-range Weather Forecasting (ECMWF), so-called Cycle 31 (ECMWF, 2007). It
240 carries the soil parameterization presented by Van den Hurk et al. (2000) and the
241 parameterized convection is described by Bechtold et al. (2004).

242

243 RACMO2.1 is used extensively for regional climate downscaling (e.g. Lenderink et al.
244 2007) and evaluation of various components of the physical parameterization (e.g.
245 Zadelhof et al. 2007). The simulation used in the present study is a regional
246 downscaling experiment focusing on the West-African monsoon area applied in the
247 context of the European Commission sponsored project ENSEMBLES (Hewitt and
248 Griggs, 2004). The domain covers the area (38.72°W , 23.32°S , 34.76°E , 38.72°N) at
249 0.44° resolution (approximately 50 km) and 40 vertical levels. In all analyses and plots
250 a boundary relaxation zone of 10 grid points on either side was excluded. The hindcast
251 simulation was carried out using ECMWF Interim Reanalysis data (Uppala et al. 2008)
252 as lateral boundary conditions for the period January 1989 – November 2007. A 3
253 year spin-up using ECMWF 40-yr Reanalysis data (Uppala et al. 2005) was applied
254 covering 1986 – 1988. From an evaluation with observed precipitation fields, an
255 apparent wet bias during the spin-up period was reduced considerably upon the
256 introduction of ERA-Interim lateral boundary conditions from 1989 onwards.
257 The soil moisture W used here is defined as the total water column in the top 1 m of
258 the soil grid, which contains 4 levels up to a depth of 2.89 m. Although stratiform and
259 convective precipitation was stored separately, only total precipitation is considered in
260 the analysis.

261

262 Although a full verification of the RCM is not the scope of this study, a decent
263 representation of the main hydrological cycle needs to be confirmed. Figure 1 shows a
264 mean seasonal spatial distribution of precipitation, compared with the Climate
265 Prediction Center (CPC) Merged Analysis of Precipitation (CMAP) data (Xie and Arkin

266 1997). Evidently both the location and order of magnitude of the seasonal mean
267 precipitation are well reproduced by the RCM. However, anomaly correlation
268 coefficients between monthly RCM and CMAP data vary across the land area between
269 0.2 and 0.6, which implies a poor reconstruction of the year-to-year variability of
270 monthly mean precipitation (not shown). Anomaly correlations between precipitation
271 from the RCM and the driving ERA-Interim data are higher near the boundaries of the
272 model domain, but drop to similarly low values in the West-African monsoon area.
273 Apparently the model has considerable degrees of freedom to adjust its interior
274 hydroclimate away from the forcing boundaries. Therefore, indicators for variability
275 and land-atmosphere interaction, under investigation here, are considered to be
276 affected by modeled atmospheric and land processes, and hardly constrained by the
277 lateral forcing.

278

279 **Regions of strong land-atmosphere interaction**

280 A strong systematic hydrological feedback between land and atmosphere requires the
281 simultaneous sensitivity of evaporation to soil moisture and of precipitation to
282 atmospheric water content (Dirmeyer 2006). In our setup areas where these
283 sensitivities occur are indicated by significant correlations between E and W and
284 between W and R .

285

286 Figure 2 shows the areas with significant correlation between E and W anomalies. In
287 the core of the heavy precipitation area around the equator the correlations tend to be
288 negative, indicating evaporation to be controlling soil moisture content (by depletion
289 of the reservoir) rather than vice versa. In the dry Sahara and Kalahari deserts the

290 correlation is weak owing to the small variability of either signal. But in a major portion
291 of the domain significant positive correlations are found. This is in broad agreement
292 with Dirmeyer et al. (2009), who base their findings on offline simulations with an
293 ensemble of land surface models driven by observed precipitation and radiative
294 forcings.

295

296 Figure 3 shows the similar plot, but for the correlation between soil moisture W and
297 recycling ratio R using $L = 500$ km. Results are very similar for recycling ratio's
298 calculated with other values of L . R is only defined when precipitation is present, which
299 precludes any coherent signal in the deserts.

300

301 The strongest and most coherent positive correlation patterns are shown in JJA in the
302 West African monsoon area, and in the seasons following the main wet period, MAM
303 and SON on the Southern hemisphere, and SON in the a region south of the Sahel.
304 The JJA monsoon signal is probably reflecting interannual variability in the spatial
305 extent of the West African monsoon. Apparently, surface moisture conditions are
306 rather variable and co-varying with the recycling ratio. High recycling ratios during wet
307 conditions imply conditions where precipitation is partly determined by local
308 evaporation; increases in water supply from the surface increase precipitation.
309 Negative correlations indicate wet soil anomalies by rainfall originating from remote
310 areas. This particularly applies to the equatorial tropics in all seasons, and a narrow
311 strip in the Sahel during SON. Again, results are similar to the findings of Dirmeyer et
312 al. (2009), including the alternating negative-positive-negative signal between 10°N
313 and the equator in SON.

314

315 In Figure 4 the areas where the correlations shown in Figures 2 and 3 are significantly
316 positive are indicated per season. Also shown is the seasonal mean soil moisture
317 memory time scale (the e-folding time scale of lagged correlations). The simultaneous
318 presence of the two positive correlations is indicative for a systematic influence of soil
319 moisture anomalies on precipitation at seasonal time scales during the 19 year
320 analysis period. This influence is strongly constrained, and basically limited to the
321 northern edge of the West-African monsoon in JJA and some scattered areas during
322 the subsequent drying stage in SON, and the equatorward edge of the monsoon in the
323 onset periods (MAM on Northern hemisphere, SON on Southern hemisphere). The
324 South-Africa area is within the influence radius of the lateral relaxation of the RCM to
325 ERA-Interim fields, which possibly introduces model tendencies that are difficult to
326 interpret in terms of atmospheric responses to land surface conditions.

327

328 In the study of Koster et al. (2004), which was confined to a single JJA season, roughly
329 the same Sahelian area is highlighted as in Figure 4. They use a coupling strength
330 diagnostic measuring the degree to which precipitation variability is affected by soil
331 moisture anomalies. In Figure 4 a different metric is plotted, but aiming at a similar
332 connection between the surface wetness and precipitation.

333

334 Further analyses of the land-atmosphere interaction using RCM model output
335 concentrate on two contrasting but sensitive areas (see boxes in Figure 4): the
336 Northern Sahel located between $12^{\circ}\text{W} - 8^{\circ}\text{E}$ and $12^{\circ}\text{N} - 17^{\circ}\text{N}$, and the inland
337 Tropical area covering Chad, Central African Republic and southern Sudan between

338 15°E – 26°E and 2°N – 8°N. The former region shows positive correlations in JJA and
339 somewhat in the subsequent drying season, whereas the latter region has low
340 correlations in all seasons but MAM. Figure 5 shows the monthly mean values of
341 evaporation and recycling ratio as function of W averaged for these two areas. Monthly
342 mean values are labeled and colored by the season. For evaporation the seasonal cycle
343 of the Sahelian area shows a larger amplitude and is shifted in time compared to the
344 Tropical domain. Evaporation gradually increases with W but a much stronger
345 sensitivity is shown in the drying cycle in the Sahel, where high radiative inputs and
346 availability of soil water cause a rapid depletion of the soil reservoir. In the tropical
347 subdomain this rapid decline of evaporation does not take place until the boreal winter
348 season (DJF), and little difference in sensitivity $\Delta E/\Delta W$ between JJA and SON is
349 observed.

350

351 For recycling ratio the situation is different. In the Sahelian area the overall recycling
352 ratio is highest in JJA, and also the sensitivity $\Delta R/\Delta W$ is only clearly positive during the
353 JJA season, allowing a systematic land – atmosphere feedback. In the tropical area a
354 strong dependence of R on W is apparent in SON, when a rapid decline of R from
355 September to November takes place. In spite of this strong dependence a lack of soil
356 moisture control on evaporation prohibits a strong land – atmosphere feedback in this
357 area during JJA and SON.

358

359 The MAM signature in the tropical and Sahelian subdomains shown in Figure 4 can
360 also be understood from a different phasing of the seasonal cycle of $\Delta E/\Delta W$ in these
361 two areas: although E strongly increases with soil water in the Sahelian spring season,

362 the limited water availability does not allow a sustained evaporation or recycling. In the
363 tropical area the wet season has clearly started by the end of MAM, and recycling
364 ratios are positively affected by additional moisture availability.

365

366 **Key surface-atmosphere relationships in interaction regions**

367 The response of the precipitation features to soil moisture anomalies is governed by
368 both land surface and atmospheric processes. While several studies have explored the
369 sensitivity of precipitation to changing land surface conditions (see references in
370 introduction), only few systematically address the atmospheric conditions that must
371 be met in order to allow a strong land-atmosphere feedback.

372

373 *Lifting Condensation Level and Convective Triggering Potential*

374 Among others, Betts (2004) use the relation between Lifting Condensation Level and
375 soil moisture to diagnose regions of strong interaction while exploring results from
376 NCEP and ECMWF reanalysis products. A strong sensitivity of the LCL to soil moisture
377 anomalies is at the origin of a number of subsequent feedbacks: boundary layer mixing
378 up to the level of free convection, cloud formation and shortwave and longwave
379 radiative responses when condensation occurs, or eventually triggering or fuelling of
380 convection.

381

382 Figure 6 (top row) shows an aggregated picture of the relation between LCL and soil
383 moisture in both subdomains. A general tendency of lower LCL with higher soil
384 moisture is evident, but both areas expose a similar asymmetric seasonal cycle, with a
385 low LCL and low sensitivity to soil moisture in the major wet season, and a steeply

386 increased LCL and sensitivity in the subsequent drying phase. Thus, in this drying
387 phase a given soil moisture anomaly has a significantly stronger impact on the LCL
388 than a similar anomaly during the period of wetting. Differences in the atmospheric
389 configuration between these two phases are apparently not only reflected in the
390 seasonal cycle of precipitation, but also in the sensitivity to the surface conditions.

391

392 A higher LCL is also positively correlated to a higher Convective Triggering Potential
393 (CTP) (Figure 6, middle row). Both CTP and LCL values are rather low and not very
394 variable during the core wet season (JJA) in both regions. Larger systematic excursions
395 are shown in both the wetting and the drying seasons. The relationship between CTP
396 and LCL is fairly similar in both seasons in the Tropical subdomain, but in the Sahelian
397 area lower LCL values are associated with enhanced CTP in the SON season,
398 presumably giving rise to easier convective triggering due to LCL rise.

399

400 The bottom row in Figure 6, showing the relation between the low level dewpoint
401 depression HI_{low} and soil moisture, reveals an important constraint on strong land-
402 atmosphere interaction during the entire seasonal cycle. For the Sahelian area HI_{low} in
403 JJA is on average confined to values < 15 K (consistent with the range found by Findell
404 and Eltahir, 2003a; see below) but quickly reaches very high values in the subsequent
405 dry season, particularly from October onwards. Although relatively small soil moisture
406 perturbations could reduce HI_{low} considerably in this steep regime, the atmosphere is
407 often too dry to form precipitation, which implies a strong constraint on the control
408 exerted by soil moisture on the precipitation formation. In the Tropical domain HI_{low}
409 stays well within the “precipitable range” < 15 K in all seasons but DJF, but the

410 variability in soil moisture conditions in particularly SON is very small due to the
411 persistent precipitation, which also reduces the impact of soil moisture anomalies on
412 regional precipitation to a minimum.

413

414 *CTP, HI_{low} and soil moisture anomalies*

415 In the CTP – HI_{low} framework of Findell and Eltahir (2003a,b), too low or too high
416 values of HI_{low} rule out any surface influence on convective triggering, as the
417 atmospheric structure is overruling any surface anomaly. In a small range of HI_{low} –
418 CTP values surface conditions do matter: low HI_{low} (between about 5 and 10K) and
419 positive CTP favor convection over wet surface conditions implying a positive feedback
420 mechanism. Higher HI_{low} values (between 10 and 15K) and CTP-values well above
421 zero are preferred for convection over dry soils. They use a modeling approach in
422 which for a given day surface wetness conditions are varied and the convective
423 response is explored. Such an experiment could be repeated with an RCM (by running
424 a small ensemble with variable soil moisture conditions around a reference run, for
425 instance applied by Fischer et al, 2007), but this experiment was not carried out for
426 the present study.

427

428 Instead, the potential role of the soil wetness condition on the atmospheric ability to
429 form precipitation has been investigated by directly relating soil moisture to the CTP –
430 HI_{low} regimes. Assuming the CTP and HI_{low} thresholds proposed by Findell and Eltahir
431 (2003a) to be generally applicable, we can separate the occasions where convection is
432 favored over wet soils from conditions with dry soil advantage or no soil control.

433 Figure 7 shows the probability of wet soil advantage conditions (p_{WSA}), defined as the

434 relative number of days in every season where $CTP > 0$ J/kg and $5 < HI_{low} < 10$ K.
435 Figure 8 shows the analogous probability p_{DSA} for atmospheric conditions with a dry
436 soil advantage ($CTP > 150$ J/kg and $10 < HI_{low} < 15$ K). Only points are shown where
437 $>5\%$ of the days in the indicated seasons are within the indicated regime. Although the
438 general applicability of the chosen thresholds may be disputed, the spatial signature of
439 the results is not very sensitive to the choice of the threshold values. Reducing for
440 instance the critical value of HI_{low} where a transition from a wet to a dry soil advantage
441 regime occurs from 10 K to 8 K obviously decreases p_{WSA} and increases p_{DSA} , but these
442 changes occur in the same domains as shown in Figures 7 and 8. In most of the
443 domain the atmospheric conditions were either in the wet soil or dry soil advantage
444 regime for more than 85% of the days when rain occurred (not shown).

445

446 In general, wet soil advantage conditions are more frequent than dry soil conditions.
447 The areas where a mixture of wet and dry favoring conditions occurs do coincide near
448 the outermost limits of the wet seasons, and dry soil advantage is barely seen in the
449 deep convective core of the rain seasons. Thus, according to this diagnostic positive
450 feedback occasions (where convection is triggered over wet soils) are more frequent
451 than negative feedback. In particular positive feedbacks remain possible in the
452 Northern edge of the Sahelian rainfall region in SON, when the major rainfall systems
453 are on their retreat southwards. However, outside the tropical rainfall zone positive
454 and negative feedback occurrences are collocated in the same areas and seasons. This
455 implies that conditions with wet or dry soil advantage do alternate, and a systematic
456 positive or negative effect of soil moisture anomalies on convective triggering is

457 difficult to be established. This introduces an extra constraint for a strong systematic
458 role in soil moisture on precipitation events.

459

460 The results show that for $CTP > 0$ relatively low near surface dewpoint depressions
461 (< 10 K) occur more often than higher values of HI_{low} . To assess whether this is related
462 to the soil moisture conditions in the RCM runs, an additional check is performed. For
463 each day where rain occurred the atmospheric condition was labeled as either wet soil
464 or dry soil advantage. The soil moisture content of the *previous* day was averaged for
465 each of these two regimes, and labeled as W_{WSA} and W_{DSA} for the soil moisture content
466 in the rainy wet soil and dry soil advantage regimes, respectively. A zero-hypothesis
467 was tested with a Student's t-test that W_{WSA} is similar to W_{DSA} . The shaded areas shown
468 in Figure 9 indicate regions where there is a 95% probability that this is not the case,
469 i.e. $W_{WSA} \neq W_{DSA}$. This is a less stringent test than to demand that $W_{WSA} > \bar{W}$ (the
470 climatological mean soil moisture content) and $W_{DSA} < \bar{W}$. To further reduce the
471 scatter in the data the same smoothing was applied as before: only locations where at
472 least 6 out of 9 adjacent grid boxes showed a significant difference of the same sign
473 are plotted.

474

475 Positive numbers support the assumption that in an atmosphere with wet soil
476 advantage conditions ($HI_{low} < 10$ K and $CTP > 0$ J/kg) precipitation is formed easier
477 when the previous-day soil moisture is higher than the soil moisture content values
478 that are associated with precipitation events occurring at dry soil advantage conditions
479 ($HI_{low} > 10$ K and $CTP > 150$ J/kg). Precipitation is then considered to be related to the
480 effect of the soil moisture content on the moistening of the lower atmosphere (wet soil

481 advantage conditions) or lifting the LCL to a sufficient height to promote convection
482 (dry soil advantage conditions). The signal shown in Figure 9 does not appear very
483 coherent. At the edges of the wet seasons statistically different soil moisture contents
484 for wet soil and dry soil advantage regimes are shown, and positive ($W_{WSA} > W_{DSA}$)
485 values are clearly dominant. In the boxes with significant positive correlations between
486 E and W and between W and R (Figure 4) the signal in Figure 9 is not covering all grid
487 points. Also, areas with significant differences between W_{WSA} and W_{DSA} are found at
488 other locations in other seasons, where Figure 4 does not point at a strong
489 atmospheric response to soil moisture anomalies.

490

491 **Discussion and conclusions**

492 We have used correlations between soil moisture, evaporation and recycling ratio
493 generated with a Regional Climate Model nested in meteorological reanalysis data
494 during a 19-year period to identify regions of potential control of surface wetness
495 conditions on rainfall in a large African domain. The correlation framework was used
496 before by Dirmeyer et al. (2009) using observations and offline model results covering
497 the entire globe. For the region of interest we find similar spatial and seasonal patterns
498 of areas where evaporation and recycling ratio are partly controlled by soil moisture:
499 the northern edge of the West-African monsoon in JJA, and a number of smaller
500 regions including a tropical Northern hemispheric region in MAM. In these regions
501 and seasons, evaporation is substantial and to some extent governed by the available
502 soil moisture content, and not only by available radiation and/or atmospheric demand
503 for water. During the dry seasons in the Sahel evaporation rates and soil moisture are
504 too low to detect a substantial correlation above the noise level, and in the heart of the

505 wet season soil moisture is abundant and not constraining evaporation. A strong
506 correlation between soil moisture and recycling ratio points at the local origin of
507 moisture for precipitation. In the tropical zones around the equator moisture advected
508 from the oceans is presumably the primary source of moisture. Away from the equator
509 significant correlations between soil moisture and recycling ratio exist during the
510 transition seasons SON and MAM.

511

512 In the regions of potential land-atmosphere interaction, we analyzed the seasonal
513 cycles and soil related variability of a number of key atmospheric variables. The Lifting
514 Condensation Level (LCL) displays a pronounced seasonal cycle in harmony with the
515 migration of the precipitation systems. Low values are associated with the wet season
516 as the soil becomes wetter, while during the drying stage LCL rapidly rises with
517 decreasing soil moisture. This rapid increase points at a strong sensitivity of the
518 atmospheric condition to soil moisture conditions. This seasonal cycle is typical for
519 every location within reach of the seasonal precipitation (either ITCZ or monsoon),
520 although the timing over the year varies with location. However, also for areas without
521 significant correlations between soil moisture, evaporation and recycling ratio this
522 asymmetry in atmospheric sensitivity to soil moisture conditions is found apparent.
523 Thus other mechanisms must be in place as well to explain a strong atmospheric
524 sensitivity to surface wetness conditions.

525

526 When rising air comes to condensation extra energy is released that may trigger moist
527 convection. From a comparison between the two key regions the relationship between
528 LCL and Convective Triggering Potential (CTP) shows a slightly different seasonal

529 signature. In the region with strong coupling in JJA (Northern Sahel) a hysteresis
530 between LCL and CTP appears: during the drying phase the LCL is lower at a given
531 CTP-value than during the wetting season MAM. This may favor the release of more
532 convective potential energy, providing a link between the soil state and the convection.
533 However, the generally dry state of the atmosphere outside the main wet season forms
534 an extra constraint on the potential role of soil moisture in convective triggering. In the
535 tropical area the LCL – CTP relation is more symmetric, and the LCL rise in the drying
536 season does not affect CTP differently.

537

538 From an evaluation of previous-day soil moisture under conditions of rainfall it was
539 seen that there are many locations where soil moisture is indeed higher for wet soil
540 advantage conditions than for dry soil advantage. However, this feature is not very
541 coherent. Wet soil advantage conditions – associated with a positive feedback as
542 precipitation is promoted under wet soil conditions – are more widespread and
543 frequent than dry soil advantage conditions, and remain present in the Northern Sahel
544 during the retreat of the rainfall in SON.

545

546 The diagnostics analyzed here do indicate a positive contribution of soil moisture
547 anomalies to the occurrence of rainfall on a climatological time scale, but in general
548 the areas where this coupling is strong are fairly small. Precipitation in the tropical
549 convergence zone and the adjacent trade wind regimes is dominated by migrating and
550 growing mesoscale precipitation systems, whose dynamics are dominated by large
551 scale atmospheric features. Local moisture anomalies may influence the activity or
552 trajectory of these rainfall mechanisms (Taylor et al, 2007), but the spatial scale at

553 which this interaction is active is probably too small to be picked up by the RCM and
554 diagnostics used in this study.

555

556 Land – atmosphere interaction is governed by a combination of surface and
557 atmospheric processes. Although the model used is only a approximation of the true
558 processes in nature and possibly shows biases with respect to the behavior of land
559 surface and convection parameterizations (e.g. Hohenegger et al, 2009), the results
560 do show that for the limited number of areas where land-atmosphere coupling is
561 found to be significant the relevant processes needed for an atmosphere to respond to
562 (anomalous) soil conditions are in place. From a statistical point of view the role of
563 surface conditions in the precipitation dynamics is generally not overwhelming, even
564 under conditions where soil moisture exerts a significant influence on surface
565 evaporation. The seasonal cycle of the atmospheric properties is an important
566 modulator of the degree to which hydrological surface anomalies extension affect the
567 precipitation formation process. A strong sensitivity of evaporation to soil moisture
568 does not lead to a response of rainfall when the atmosphere is too dry to form
569 precipitation. However, the study focuses on systematic land – atmosphere interaction
570 with a climatological perspective. The small values of the general statistical
571 correlations found in the 19-year time record do not preclude the existence of short
572 anomalous episodes when soil moisture conditions do have a strong effect on local
573 precipitation. A similar contradiction can be formulated for Central European summer
574 conditions: in the systematic analyses of Koster et al. (2004) and Dirmeyer et al.
575 (2009) the mean impact of soil moisture anomalies on summertime precipitation are
576 small, but extreme events like the 2003 heatwave have triggered many studies that

577 highlighted the importance of the land – atmosphere feedback in maintaining the
578 anomalous conditions (e.g. Ferranti and Viterbo 2006).

579

580 The study was designed to demonstrate a number of diagnostics that in principle
581 could be observed, and do not require model sensitivity runs like the set-up of Findell
582 and Eltahir (2003a), Koster et al. (2004) and Hohenegger et al. (2009). However,
583 further work is needed to verify the RCM results with true observations. Also the
584 diagnostic framework could still be developed further. We already referred to the
585 importance of quantifying conditional predictability in cases where systematic land –
586 atmosphere interaction is small but where during individual episodes a strong soil
587 control on the regional hydrological cycle may exist. Also, diagnostics that – other than
588 this study – measure the potential influence of anomalous soil moisture conditions on
589 precipitation in remote areas (see e.g. the case studies by Beljaars et al. 1996;
590 Haarsma et al. 2009) remains a relevant topic for research.

591

592 **Acknowledgements**

593 The RCM runs are carried out under the auspices of the ENSEMBLES project (see
594 <http://www.ensembles-eu.org>). Geert Lenderink has presented results from this study
595 to other groups participating in ENSEMBLES. A land-atmosphere coupling workshop
596 co-sponsored by the GEWEX panel GLASS (www.gewex.org/glass.html) and the EU-
597 project WATCH (<http://www.eu-watch.org>) in De Bilt in June 2008 gave a lot of
598 inspiration for this study. CMAP Precipitation data were provided by the
599 NOAA/OAR/ESRL PSD, Boulder, Colorado, USA, from their web site at
600 <http://www.cdc.noaa.gov>.

601

602 **References**

- 603 D'Andrea, F., A. Provenzale, R. Vautard and N. De Noblet, 2006: Hot and cool summers: multiple
604 equilibria of the continental water cycle. *Geophys. Res. Lett.*, **33**, L24807.
- 605 Bechtold, P., J.-P. Chaboureaud, A. Beljaars, A.K. Betts, M. Köhler, M. Miller and J.-L. Redelsperger, 2004:
606 The simulation of the diurnal cycle of convective precipitation over land in a global model. *Q.J.R.*
607 *Meteorol. Soc.*, **130**, 3119-3137.
- 608 Beljaars, A.C.M., P. Viterbo, M.J. Miller and A.K. Betts, 1996: The anomalous rainfall over the USA
609 during July 1993: Sensitivity to land surface parametrization and soil moisture anomalies.
610 *Mon. Wea. Rev.*, **124**, 362-383.
- 611 Betts, A.K., 2004: Understanding hydrometeorology using global models. *Bull. Am. Met. Soc.*, **85**, 1673-
612 1688.
- 613 Bierkens, M.P. and B.J.J.M. van den Hurk, 2007: Groundwater convergence as a possible mechanism
614 for multi-year persistence in rainfall. *Geophys. Res. Lett.*, **34**, doi:10.1029/2006GL028396.
- 615 Bisselink, B. and A.J. Dolman, 2008: Precipitation recycling: moisture sources over Europe using ERA40
616 data. *J. Hydrometeorol.*, **9**, 1073-1083.
- 617 Cook, B.I., G.B. Bonan and S. Levis, 2006: Soil moisture feedbacks to precipitation in Southern Africa. *J.*
618 *Climate*, **19**, 4198-4206.
- 619 Dirmeyer, P. A., 2006: The hydrologic feedback pathway for land-climate coupling. *J. Hydrometeorol.*, **7**,
620 857-867.
- 621 Dirmeyer, P.A., C.A. Schlosser and K.L. Brubaker, 2009: Precipitation, recycling and land memory: an
622 integrated analysis. *J. Hydrometeorol* (in press), DOI: 10.1175/2008JHM1016.1.
- 623 Dirmeyer, P.A., R.D. Koster and Z. Guo, 2006: Do global models properly represent the feedback
624 between land and atmosphere. *J. Hydromet.*, **7**, 1177-1197.
- 625 Dominguez, F., P. Kumar, X.-Z. Liang and M. Ting, 2006: Impact of atmospheric moisture storage on
626 precipitation recycling. *J. Climate*, **19**, 1513-1530.

627 Douville, H., S. Conil, S. Tyteca and A. Voltaire, 2007: Soil moisture memory and West-African
628 monsoon predictability: artefact or reality? *Climate Dynamics*, DOI 10.1007/s00382-006-0208-
629 8.

630 Douville, H., 2009: Relative contribution of soil moisture and snow mass to seasonal climate
631 predictability: a pilot study. *Climate Dynamics* (in press)

632 ECMWF, 2007: *IFS Documentation*. see <http://www.ecmwf.int/research/ifsdocs/CY31r1>.

633 Ferranti, L. and P. Viterbo, 2006: The European summer of 2003: sensitivity to soil water initial
634 conditions. *J. Climate*, **19**, 3659-3680.

635 Findell, K.L. and E.A.B. Eltahir, 2003a: Atmospheric control on soil moisture-boundary layer
636 interactions; Part I: Framework development. *J. Hydrometeorol.*, **4**, 552-569.

637 Findell, K.L. and E.A.B. Eltahir, 2003b: Atmospheric control on soil moisture-boundary layer
638 interactions; Part II: Feedbacks within the continental United States. *J. Hydrometeorol.*, **4**, 570-
639 583.

640 Fischer, E.M., S.I. Seneviratne, P.L. Vidale, D. Luthi and C. Schär, 2007: Soil Moisture-Atmosphere
641 interactions during the 2003 European summer heatwave. *J. Climate*, **20**, 5081-5099.

642 Guo, Z., P. A. Dirmeyer, R. D. Koster, G. Bonan, E. Chan, P. Cox, H. Davies, T. Gordon, S. Kanae, E.
643 Kowalczyk, D. Lawrence, P. Liu, S. Lu, S. Malyshev, B. McAvaney, K. Mitchell, T. Oki, K. Oleson,
644 A. Pitman, Y. Sud, C. Taylor, D. Verseghy, R. Vasic, Y. Xue, and T. Yamada, 2006: GLACE: The
645 Global Land-Atmosphere Coupling Experiment. 2. Analysis. *J. Hydrometeorol.*, **7**, 611-625.

646 Haarsma, R.J., F.M. Selten, B.J.J.M. van den Hurk, W. Hazeleger and X. Wang, 2009: Drier Mediterranean
647 Soils due to Greenhouse Warming bring easterly Winds over Summertime Central Europe.
648 *Geophys. Res. Lett.*, **36**, L04705, doi:10.1029/2008GL036617.

649 Hewitt, C. D. and D. J. Griggs, 2004: Ensembles-based Predictions of Climate Changes and their
650 Impacts. *Eos*, **85**, p566; see also <http://www.ensembles-org.uk>.

651 Hohenegger, C., P. Brockhaus, C. S. Bretherton and C. Schär, 2009: The soil moisture-precipitation
652 feedback in simulations with explicit and parameterized convection. *J. Climate* (in press).

653 Kanamitsu, M. and C. Mo, 2003: Dynamical effects of land surface processes on summer precipitation
654 over the Southwestern United States. *J. Climate*, **16**, 496-509.

655 Koster, Randal D., Max J. Suarez, Mark Heiser, 2000: Variance and Predictability of Precipitation at
656 Seasonal-to-Interannual Timescales. *J. Hydromet.*, **1**, 26-46.

657 Koster, R. D., M. J. Suarez, R. W. Higgins, and H. M. Van den Dool, 2003: Observational evidence that
658 soil moisture variations affect precipitation. *Geophys. Res. Lett.*, **30**, 1241,
659 doi:10.1029/2002GL016571.

660 Koster, R.D., P.A. Dirmeyer, Zh. Guo, G. Bonan, E. Chan, P. Cox, C. T. Gordon, S. Kanae, E. Kowalczyk, D.
661 Lawrence, P. Liu, C-H. Lu, S. Malyshev, B. McAvaney, K. Mitchell, D. Mocko, T. Oki, K. Oleson, A.
662 Pitman, Y. C. Sud, C. M. Taylor, D. Verseghy, R. Vasic, Y. Xue, and T. Yamada, 2004: Regions of
663 Strong Coupling Between Soil Moisture and Precipitation. *Science*, **305**, 1138-1140.

664 Lenderink, G., A. van Ulden, B. van den Hurk and E. van Meijgaard, 2007: Summertime inter-annual
665 temperature variability in an ensemble of regional model simulations: analysis of the surface
666 energy budget; *Clim.Dyn.*, **29**, 2, 157-176, doi:10.1007/s00382-007-0227-z.

667 Schär, C., D. Luthi, U. Beyerle and E. Heise, 1999: The soil-precipitation feedback: a process study with
668 a regional climate model. *J. Climate*, **12**, 722-741.

669 Seneviratne, S.I., D. Luthi, M. Litschi and C. Schär, 2006: Land-atmosphere coupling and climate
670 change in Europe. *Nature*, **443**, 205-209.

671 Taylor, C.M. and R.J. Ellis, 2006: Satellite detection of soil moisture impacts on convection at the
672 mesoscale. *Geophys.Res.Lett.*, **33**, L03404.

673 Taylor, C.M., D.J. Parker and P.P. Harris, 2007: An observational case study of mesoscale atmospheric
674 circulations induced by soil moisture. *Geophysical Research Letters*, **34**, L15801.

675 Uppala et al., 2005: The ERA-40 re-analysis. *Quart. J. R. Meteorol. Soc.*, **131**, 2961-3012.

676 Uppala, S., D. Dee, S. Kobayashi, P. Berrisford and A. Simmons, 2008: Towards a climate data
677 assimilation system: status update of ERA-Interim. *ECMWF Newsletter*, **115**, 12-18. See
678 <http://www.ecmwf.int/publications/newsletters/pdf/115.pdf>

679 Van den Hurk, B.J.J.M. and E.M. Blyth, 2008: WATCH/LoCo workshop report. *Gewex newsletter*
680 2008, 12-14.

681 Van den Hurk, B.J.J.M., P. Viterbo, A.C.M. Beljaars and A.K. Betts, 2000: *Offline validation of the ERA40*
682 *surface scheme*. ECMWF TechMemo 295; see
683 <http://www.knmi.nl/publications/fulltexts/tm295.pdf>.

684 Van Meijgaard, E., L.H. van Ulf, W.J. van de Berg, F.C. Bosveld, B.J.J.M. van den Hurk, G. Lenderink,
685 A.P. Siebesma, 2008: *The KNMI regional atmospheric climate model RACMO, version 2.1*. KNMI
686 Technical Report 302, 43 pp. Available from KNMI, PO Box 201, 3730 AE, De Bilt, The
687 Netherlands.

688 Xie and Arkin, 1997: Global Precipitation: A 17-year monthly analysis based on gauge observations,
689 satellite estimates, and numerical model outputs. *Bulletin of the American Meteorological Society*,
690 **78**, 2539-2558.

691 Zadelhoff, G.J. van, E. van Meijgaard, D.P. Donovan, W.H. Knap en R. Boers, 2007. Sensitivity of the
692 shortwave radiative budget to the parameterization of ice crystal effective radius. *J. Geophys. Res.*,
693 **112**, 1-11.

694

695 **Figure captions**

696 Figure 1: RCM Modeled (top row) and CMAP observed (bottom row) seasonal mean
697 precipitation for 1989 – 2007 (mm/day). Only land points are shown. RCM data have
698 a spatial resolution of $0.44^\circ \times 0.44^\circ$, and CMAP data are at $2.5^\circ \times 2.5^\circ$.

699

700 Figure 2: Areas with significant correlations between monthly evaporation and soil
701 moisture anomalies. Plotted are areas with a 95% significant correlation between all
702 monthly values in 1989 – 2007 in DJF (upper left), MAM (upper right), JJA (lower left)
703 and SON (lower right). A spatial smoothing was applied that only masks locations
704 where $< 2/3$ of all neighboring grid boxes show significant correlations of the same
705 sign.

706

707 Figure 3: As Figure 2, but for correlations between soil moisture content W and
708 recycling ratio R ($L = 500$ km).

709

710 Figure 4: Soil memory (days) in regions with significantly positive correlations between
711 E and W (fig 2) and between R and W (fig 3), for each season. The indicated boxes
712 denote the domains used for further analyses.

713

714 Figure 5: Monthly mean values of (top) evaporation versus W and (bottom) recycling
715 ratio versus W averaged for (left) the Sahel domain and (right) the Tropical domain
716 (see boxes in Figure 4). Every number indicates a month in the year. Colors refer to the
717 main seasons (purple = DJF, red = MAM, blue = JJA, green = SON).

718

719 Figure 6: Top row: as Figure 5, for the height of the Lifting Condensation Level above
720 the surface. Middle row: monthly mean LCL plotted against Convective Triggering
721 Potential. Bottom row: HI_{low} versus soil moisture content. Note that DJF and March
722 HI_{low} values are outside the plot scale in the Sahelian region.

723

724 Figure 7: Frequency of occasions where wet soil conditions are favorable to trigger
725 convection, diagnosed from $5 < HI_{low} < 10$ K and $CTP > 0$ J/kg. Shown are relative
726 number of days per season, p_{WSA} . Note the non-linear color scale.

727

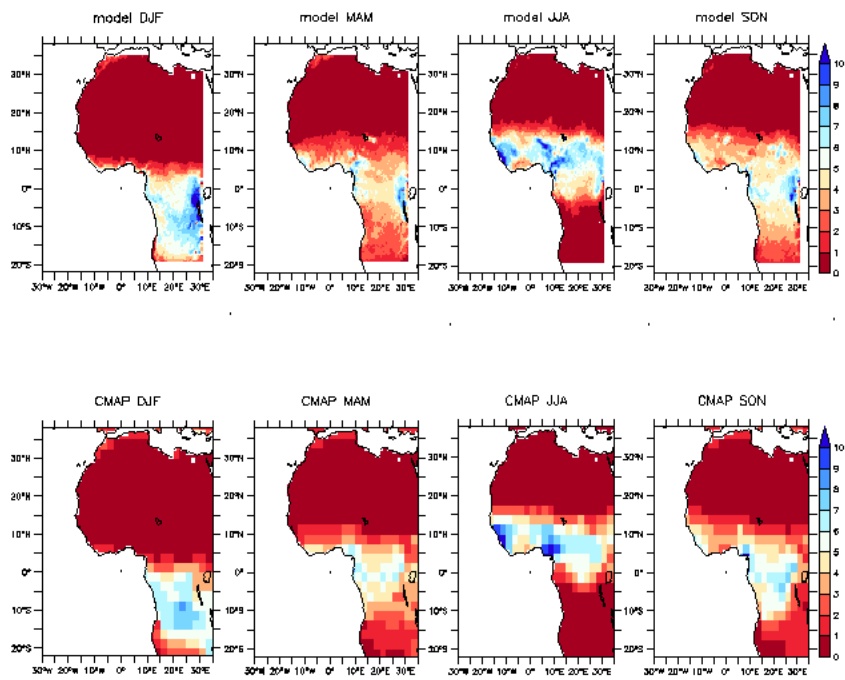
728 Figure 8: As figure 7 for dry soil conditions favoring convective triggering (p_{DSA} , $10 <$
729 $HI_{low} < 15$ K, $CTP > 150$ J/kg)

730

731 Figure 9: Significant difference between previous day soil moisture content for cases
732 where CTP and HI_{low} indicate wet soils to favor convective triggering and cases with a
733 dry soil advantage ($W_{WSA} - W_{DSA}$). A two-sided t-test (95%), and a spatial filter (≥ 6 out
734 of 9 adjacent grid boxes required to have the same significant sign) are used to mask
735 insignificant differences. The boxes shown in Figure 4 are added for geographical
736 reference.

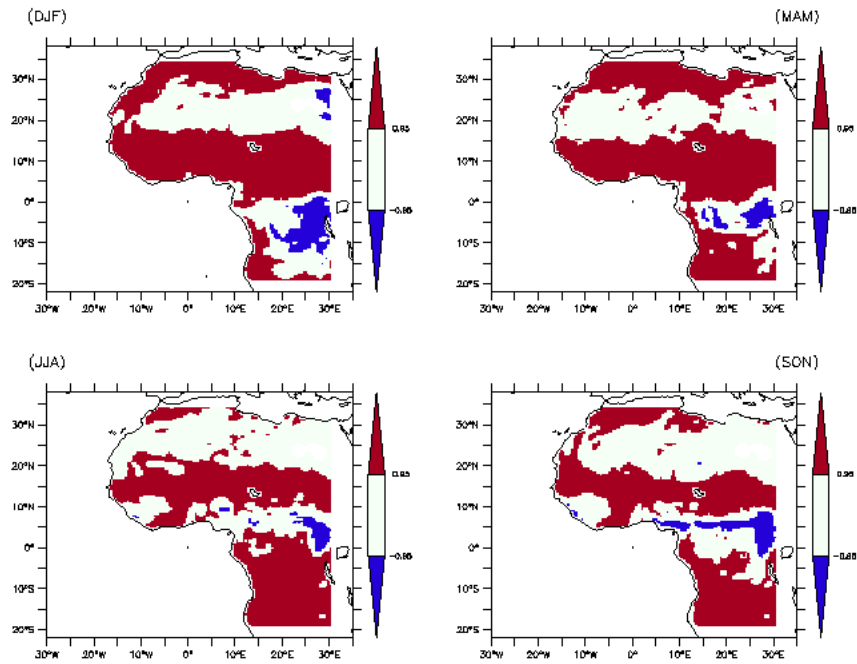
737

738 **Figures**



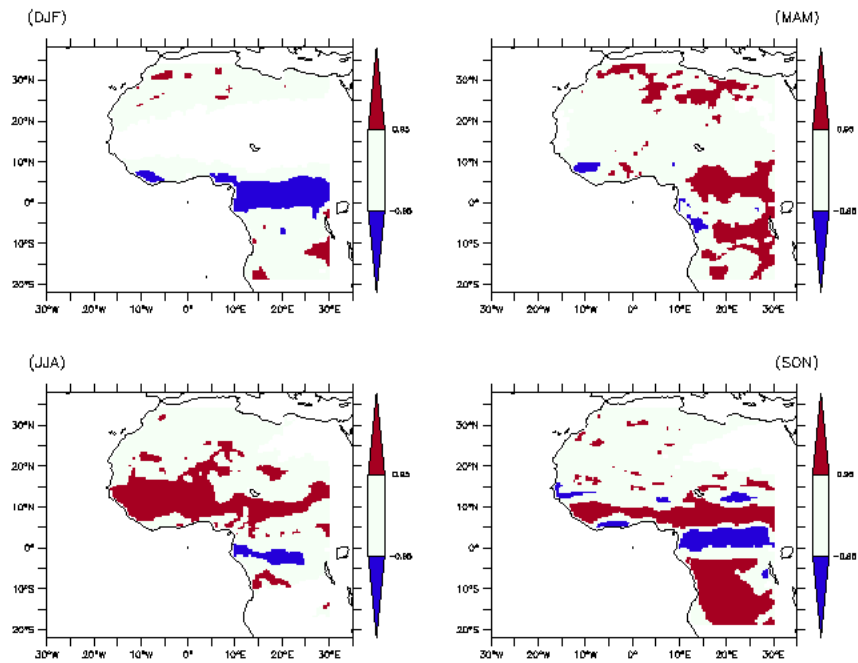
739

740 *Figure 1: RCM Modeled (top row) and CMAP observed (bottom row) seasonal mean*
741 *precipitation for 1989 – 2007 (mm/day). Only land points are shown. RCM data have a*
742 *spatial resolution of $0.44^\circ \times 0.44^\circ$, and CMAP data are at $2.5^\circ \times 2.5^\circ$.*



743

744 *Figure 2: Areas with significant correlations between monthly evaporation and soil moisture*
 745 *anomalies. Plotted are areas with a 95% significant correlation between all monthly values*
 746 *in 1989 – 2007 in DJF (upper left), MAM (upper right), JJA (lower left) and SON (lower*
 747 *right). A spatial smoothing was applied that only masks locations where <2/3 of all*
 748 *neighboring grid boxes show significant correlations of the same sign.*

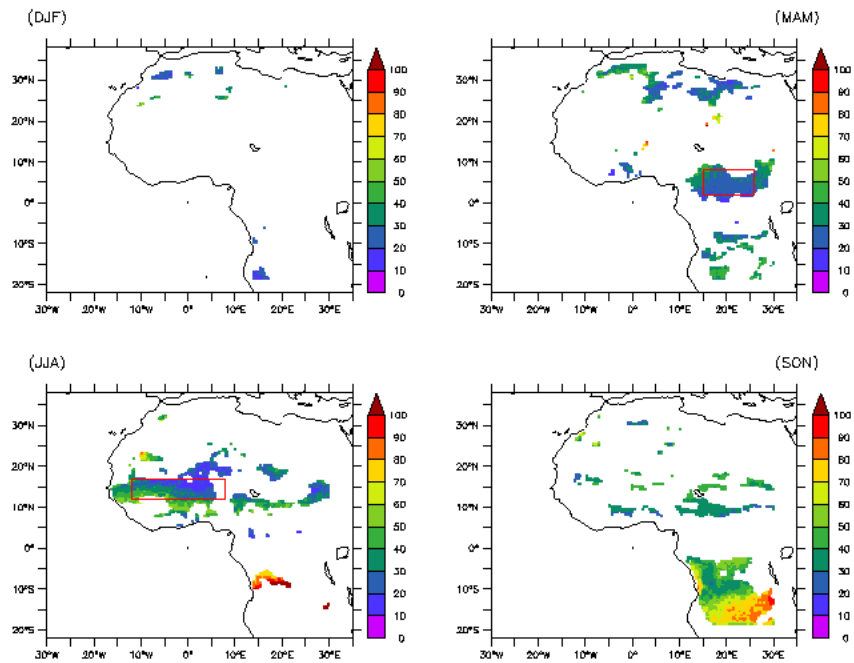


749

750

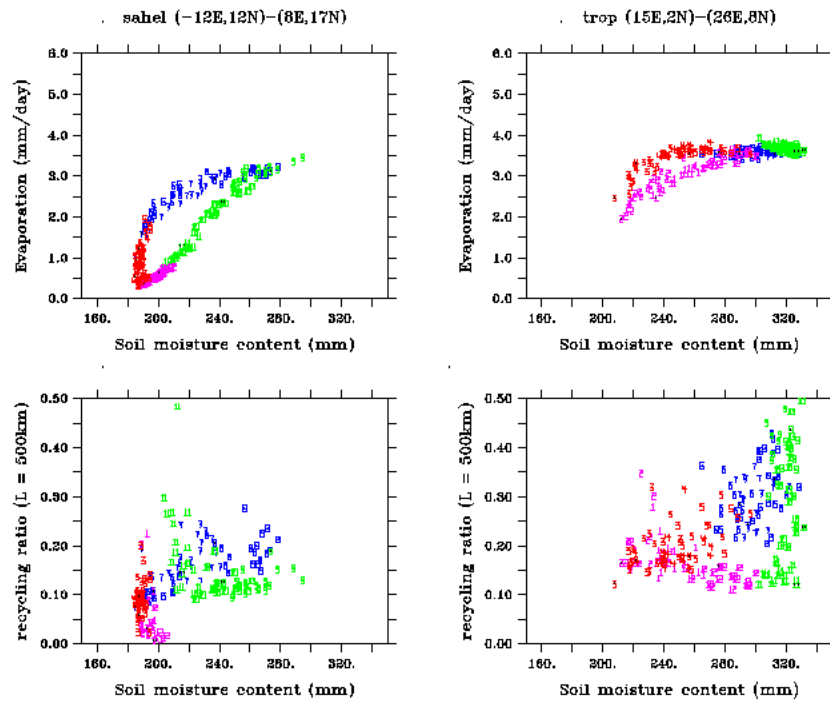
751

Figure 3: As Figure 2, but for correlations between soil moisture content W and recycling ratio R ($L = 500$ km).



752

753 *Figure 4: Soil memory (days) in regions with significantly positive correlations between E*
 754 *and W (fig 2) and between R and W (fig 3), for each season. The indicated boxes denote*
 755 *the domains used for further analyses.*

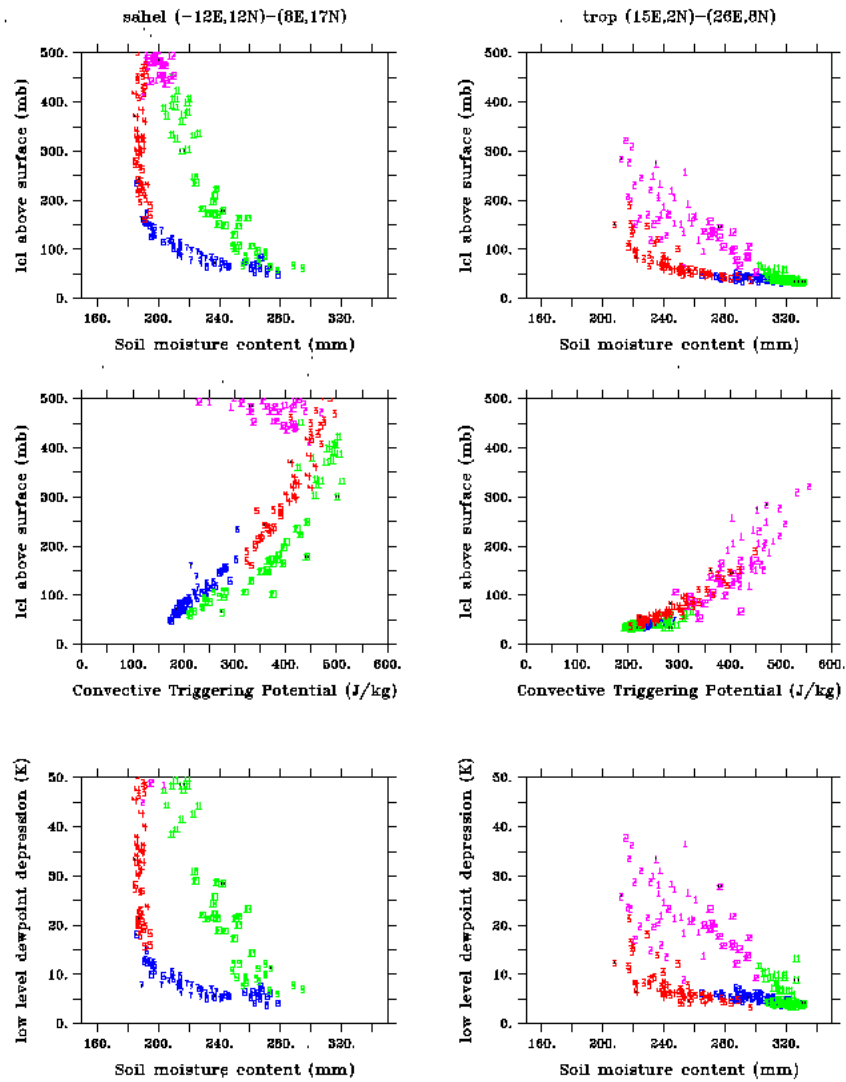


756

757 *Figure 5: Monthly mean values of (top) evaporation versus W and (bottom) recycling ratio*
 758 *versus W averaged for (left) the Sahel domain and (right) the Tropical domain (see boxes in*
 759 *Figure 4). Every number indicates a month in the year. Colors refer to the main seasons*

760

(purple = DJF, red = MAM, blue = JJA, green = SON).



761

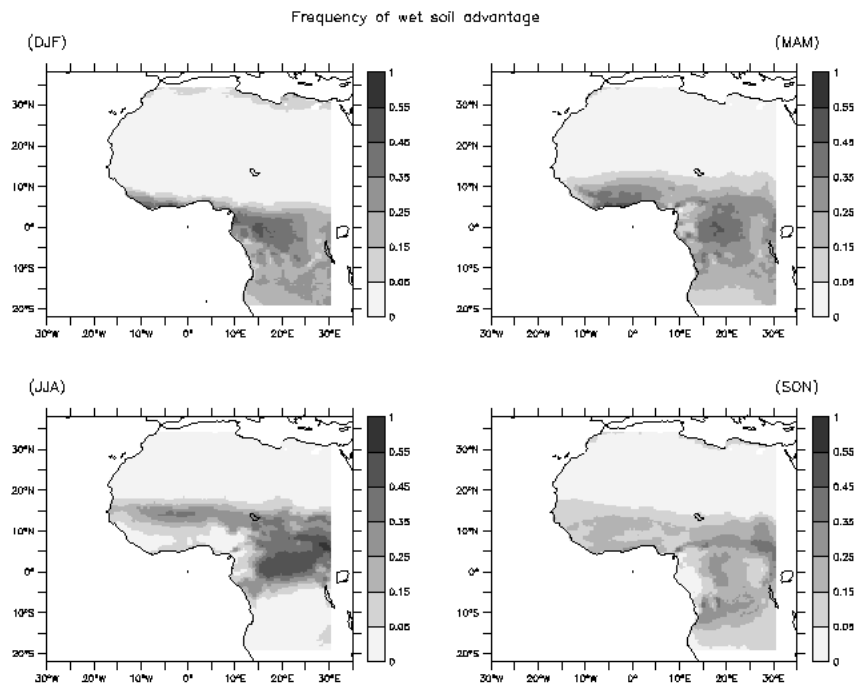
762

763 *Figure 6: Top row: as Figure 5, for the height of the Lifting Condensation Level above the*

764 *surface. Middle row: monthly mean LCL plotted against Convective Triggering Potential.*

765 *Bottom row: HI_{low} versus soil moisture content. Note that DJF and March HI_{low} values are*

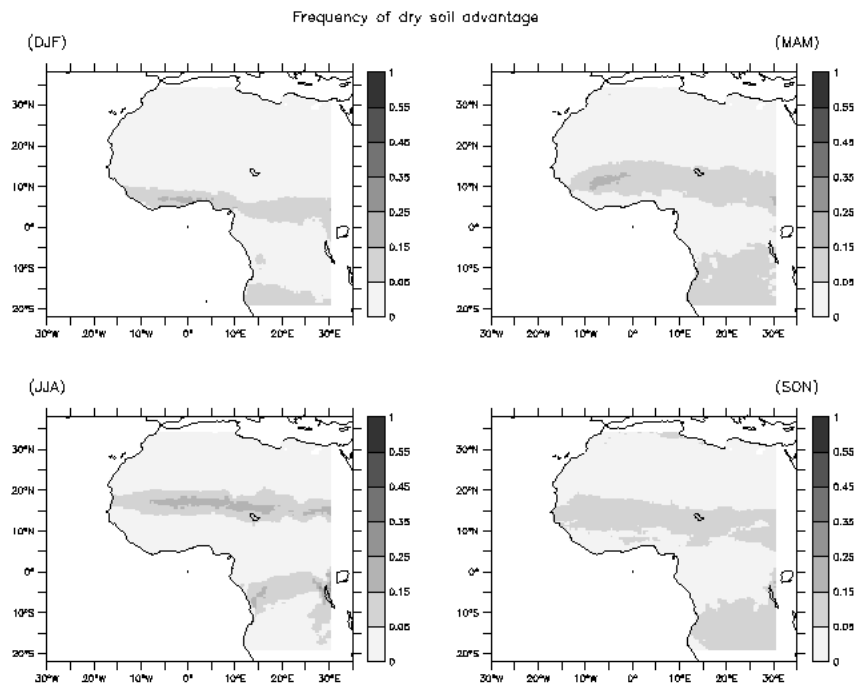
766 *outside the plot scale in the Sahelian region.*



767

768 *Figure 7: Frequency of occasions where wet soil conditions are favorable to trigger*
 769 *convection, diagnosed from $5 < HI_{low} < 10$ K and $CTP > 0$ J/kg. Shown are relative number*
 770 *of days per season, p_{WSA} . Note the non-linear color scale.*

771



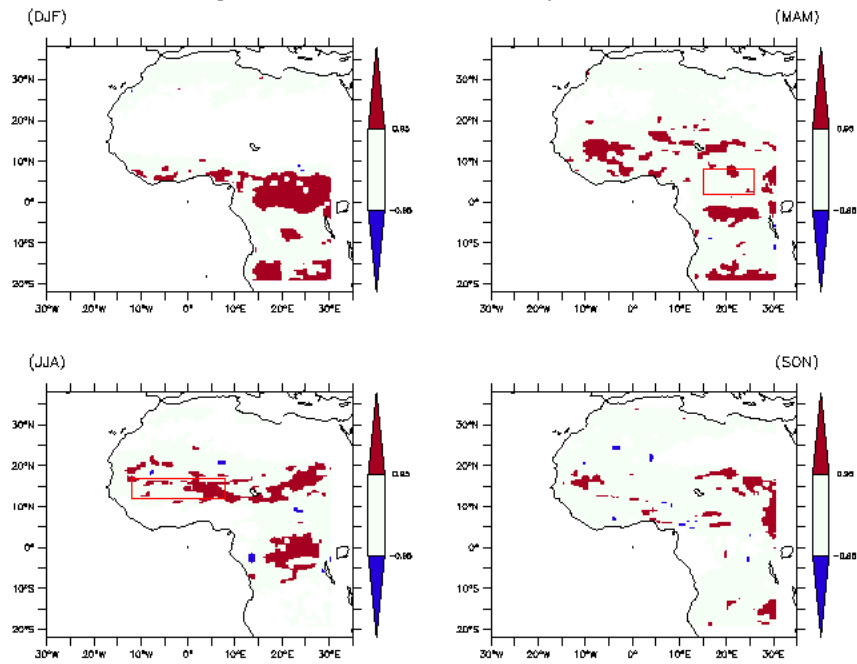
772

773 *Figure 8: As figure 7 for dry soil conditions favoring convective triggering (p_{DSA} , $10 < HI_{low} <$*

774

15 K, $CTP > 150$ J/kg)

775



776

777 *Figure 9: Significant difference between previous day soil moisture content for cases where*

778 *CTP and HI_{low} indicate wet soils to favor convective triggering and cases with a dry soil*

779 *advantage ($W_{WSA} - W_{DSA}$). A two-sided t-test (95%), and a spatial filter (≥ 6 out of 9*

780 *adjacent grid boxes required to have the same significant sign) are used to mask*

781 *insignificant differences. The boxes shown in Figure 4 are added for geographical reference.*

782